Standard enthalpies of formation of 5d aluminides by high-temperature direct synthesis calorimetry

S. V. Meschel and O. J. Kleppa

James Franck Institute, University of Chicago, 5640 S. Ellis Ave., Chicago, IL 60637 (USA)

Abstract

The standard enthalpies of formation of aluminides in the binary systems La–Al, Hf–Al, Ta–Al, W–Al, Re–Al and Pt–Al were determined by direct synthesis calorimetry at 1473 ± 2 K. The results are compared with earlier experimental data and with predicted values from Miedema's semi-empirical model. In systematic plots the enthalpies of formation of 5d aluminides are compared with similar data for the 3d and 4d aluminides, and with enthalpy data for the 5d borides, germanides and silicides.

1. Introduction

The alloys of aluminium with transition metals are of considerable theoretical and technological interest. The stability and chemical bonding in these compounds have received considerable theoretical attention in recent years [1–7]. There has also been some experimental work on the thermodynamic properties of aluminides, mostly focused on the alloys of aluminum with the 3d transition metals [8, 9]. A fairly recent review of much of this work is provided by Desai [10].

Very recently we have reported new enthalpies of formation for some 4d transition metal aluminides determined by direct synthesis calorimetry [11]. In other recent communications from this laboratory we have also published enthalpy data for some 5d aluminides, notably $LaAl_2$ and PtAl [12], as well as OsAl and IrAl [13]. The heats of formation of these compounds were also measured by direct synthesis calorimetry. In this study we present new thermochemical data for other 5d transition metal aluminides in the Hf–Al, Ta–Al, W–Al and Re–Al systems. Apart from this we have also measured the enthalpies of formation of La_3Al_{11}, Pt_3Al and Pt_2Al_3, phases which were not covered in the earlier study by Jung *et al.* [12]. Our new values complete the enthalpy of formation picture for important phases among the 5d transition metal aluminides and allow us to make systematic comparisons with other aluminide systems. We compare our results with existing data in the literature, corresponding values for the 3d and 4d transition metal aluminides, the 5d borides, germanides and silicides and predicted values from Miedema's semi-empirical model [7].

2. Experimental details and materials

The experiments were carried out at 1473 ± 2 K in a single unit differential microcalorimeter which has been described in an earlier communication from this laboratory [14]. All the experiments were performed under a protective atmosphere of argon which was purified by passing the gas over titanium powder at 900 °C. A boron nitride (BN) crucible was used to contain the samples.

Table 1 summarizes the metallic purity and particle size of the materials used in this study. All the metal samples were purchased from Johnson Matthey/AESAR. The lanthanum powder used was freshly filed from an ingot a few minutes before the measurement was initiated. The other metals were used in the powder form as purchased. All the pure components, except the highly reactive lanthanum metal, were tested by X-ray diffraction prior to use in order to detect oxide

TABLE 1. Metallic purity and particle size of the elements used in the calorimetric measurements

Element	Purity (%)	Particle size (mesh)	Comment
La	99.9	−80	Filed from ingot
Hf[a]	99.6	−325	Powder
Ta	99.98	−325	Powder
W	99.9	12 μm	Powder
Re	99.99	−325	Powder
Pt	99.99	−200	Powder
Al	99.5	−325	Powder

[a]According to Johnson Matthey the hafnium powder contains 2%–3.5% Zr by weight.

contamination or other impurities. No contamination was found. However, the hafnium sample was known to contain 2%–3.5% zirconium.

The powdered elements were carefully mixed in the appropriate molar ratio, pressed into pellets (diameter, 4 mm) and dropped into the calorimeter from room temperature. In a subsequent set of experiments the reaction products were dropped into the calorimeter to measure the heat contents of the compounds.

Calibration was performed by dropping weighed pieces of high-purity copper wire (diameter, 2 mm) from room temperature into the calorimeter at 1473 ± 2 K. The enthalpy of pure copper at this temperature, 46 435 J mol^{-1}, was obtained from Hultgren et al. [15]. The calibrations were reproducible within $\pm 1.2\%$.

3. Measurements and results

The standard enthalpies of formation of the 5d aluminides were obtained from the difference between the results of two sets of measurements. In the first set the following reaction took place in the calorimeter

$$Me \ (s, 298 \ K) + mAl \ (s, 298 \ K) \qquad (1)$$
$$= MeAl_m \ (s, 1473 \ K)$$
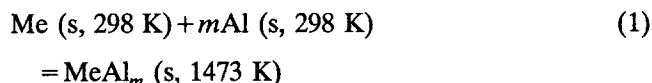
where m represents the molar ratio Al/Me, Me is the metal considered and s denotes solid. The reacted aluminide pellets were reused in a subsequent set of measurements to determine the heat contents

$$MeAl_m \ (s, 298 \ k) = MeAl_m \ (s, 1473 \ K) \qquad (2)$$
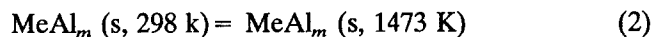
The standard enthalpy of formation is given by

$$\Delta H_f^\circ = \Delta H_m(1) - \Delta H_m(2) \qquad (3)$$

where $\Delta H_m(1)$ and $\Delta H_m(2)$ are the molar enthalpy changes associated with reactions (1) and (2).

The aluminide samples were examined by X-ray powder diffraction analysis to assess their structures and to ascertain the absence of unreacted metals. In addition, most samples were also subjected to scanning electron microscopy (SEM) and X-ray microprobe analyses.

Of the 5d transition metal–aluminum systems, we studied compounds from Hf–Al, Ta–Al, W–Al and Re–Al. The phase diagram of Hf–Al [16] shows four congruent melting intermetallic phases: Hf_3Al_2, HfAl, $HfAl_2$ and $HfAl_3$. Of these phases we carried out direct synthesis experiments on the last three. The X-ray diffraction patterns of all the three compounds were consistent with the ASTM powder diffraction file. The $HfAl_2$ compound showed complete absence of other phases, while the patterns for HfAl and $HfAl_3$ indicated trace quantities of a second phase, which for $HfAl_3$

was found to be $HfAl_2$. SEM and energy-dispersive X-ray micro-analysis confirmed that $HfAl_2$ and $HfAl_3$ were essentially single phase, while the HfAl sample showed 2%–3% of Hf_3Al_2 and Hf_4Al_5. This analysis also confirmed the presence of 6–7 at.% Zr in all the Hf samples.

The Ta–Al phase diagram shows several peritectically formed compounds [16], including Ta_2Al, TaAl and $TaAl_3$. However, in the diagram of Schuster [17] TaAl is missing and $TaAl_3$ is shown to be congruently melting at 1900 K.

We carried out direct synthesis experiments on alloy compositions corresponding to the three mentioned above. For Ta_2Al and $TaAl_3$ the experiments were successful, and generated compounds with X-ray diffraction patterns consistent with the ASTM index. There is no reported structure for TaAl in the ASTM powder diffraction file. The structure listed at TaAl corresponds to a composition of approximately 40 mol.% Al. The structure of TaAl is not listed in Massalski et al. [16] or in Pearson's Handbook [18] and hence it was not possible to generate a computer-simulated diffraction pattern. Since we cannot make a clear conclusion as to the identity of the phase, no results are reported for this sample.

SEM and energy-dispersive X-ray analysis were carried out only on the two successful samples. This analysis showed that the compound $TaAl_3$ contained the minor phases Ta_4Al and $TaAl_2$ in a total amount of less than 5%. This is not significant within our limits of error. Ta_2Al showed the presence of 3%–10% of essentially unreacted Ta metal. For this reason we consider our result for this compound to be indicative i.e. subject to possible improvement by the use of another calorimetric method.

The W–Al phase diagram shows the existence of a peritectically formed phase with the approximate composition WAl_4; this phase is stable up to about 1327 °C, i.e. above the temperature of the calorimeter [16]. We carried out direct synthesis experiments at this composition and generated this compound. Since the X-ray diffraction pattern of WAl_4 is not available in the ASTM powder diffraction file, we generated the pattern by computer simulation using the unit cell parameters and the atomic coordinates [19]. Our pattern matched the generated pattern well. SEM confirmed that the product was single phase.

There is no established phase diagram for Re–Al [16]. However, three compounds, Re_2Al, ReAl and Re_4Al_{11}, have well characterized structures [20, 21]. We attempted to prepare these three compounds by direct synthesis at 1200 °C. However, we were unable to obtain a single phase of ReAl. However, the X-ray diffraction pattern of Re_2Al matched well the pattern in the ASTM powder diffraction index. Since the dif-

fraction pattern for Re_4Al_{11} was not available in that file, we generated it by computer simulation on the basis of the unit cell parameters and the atomic coordinates [20]. We found good agreement with the calculated pattern. SEM and X-ray microprobe analysis of Re_2Al showed the presence of some Re_3Al_2 and ReAl, while the sample of Re_4Al_{11} was found to contain less than 5% ReAl.

The enthalpy of formation of $LaAl_2$ was measured by Jung et al. [12]. However, the La–Al phase diagram shows the existence of a second congruently melting stable phase, La_3Al_{11} [16], whose crystal structure was determined by Gomes de Mesquita and Buschow [22]. We prepared samples of this compound from freshly filed lanthanum metal immediately prior to each calorimetric experiment. The X-ray diffraction pattern of this phase showed excellent agreement with the ASTM X-ray diffraction file.

The Al–Pt phase diagram shows the existence of three congruent melting phases with melting points above 1500 °C: Pt_2Al_3, PtAl and Pt_3Al. Of these phases the enthalpy of formation of PtAl was determined by Jung et al. [12], who found a value in good agreement with the earlier results of Ferro et al. [23]. We prepared Pt_3Al and Pt_2Al_3 by direct synthesis calorimetry. The X-ray diffraction pattern of Pt_3Al matched well the pattern in the ASTM powder diffraction file. Since the pattern of Pt_2Al_3 was not available in that file, we generated a pattern by computer simulation from the unit cell parameters and the atomic coordinates [24]. Our experimental pattern matched well the angles in the generated pattern; however, the intensities did not correlate well. SEM and X-ray microprobe analysis indicated that Pt_3Al was single phase, while the results for Pt_2Al_3 showed the presence of a small amount of PtAl, estimated at less than 5%.

4. Results and discussion

The experimental results are summarized in Table 2. The heat effects associated with the reactions $(\Delta H_m(1))$ and the heat contents of the products $(\Delta H_m(2))$ (in kJ $(g\ atom)^{-1}$) are given as the average values of five to seven experiments with the appropriate standard deviations. The last column of this table shows the standard enthalpies of formation of the considered compounds.

Table 3 presents a comparison of the enthalpy of formation data reported in this study with experimental values from the published literature and predicted values from Miedema's semi-empirical model [7, 25]. Our values for La_3Al_{11}, $TaAl_3$, Pt_3Al and Pt_2Al_3 agree fairly well with earlier calorimetric data [9, 23, 27]; the values for La_3Al_{11} and Pt_2Al_3 are particularly close. There is

also reasonable agreement with earlier enthalpy estimates for La_3Al_{11} derived from e.m.f. data [26], for HfAl, $HfAl_2$ and $HfAl_3$ obtained from phase equilibrium studies [28] and for $TaAl_3$ and Ta_2Al from vapor pressure measurements [29]. It should be noted that the data cited earlier for the La–Al system are reported for $LaAl_4$ [26, 27] rather than for La_3Al_{11}.

We found no experimental enthalpy of formation data in the literature for WAl_4, Re_2Al and Re_4Al_{11}. Table 3 shows that there is reasonable agreement between our experimental enthalpy values and Miedema's predictions for $TaAl_3$, WAl_4 and Re_2Al. However, for La_3Al_{11}, HfAl, $HfAl_2$ and $HfAl_3$ the predicted values are considerably more exothermic than the experimental data. We found similar deviations for the enthalpies of formation of Zr–Al, Y_3Al_2 and 4d and 5d transition metal borides [11, 30, 31]. On the other hand, the predicted enthalpy values are considerably less exothermic than the measured values for Re_4Al_{11}, Pt_3Al and Pt_2Al_3. We observed similar deviations for the enthalpies of formation of compounds in the Nb–Al and Mo–Al systems and for Pd_2Al [11].

In Fig. 1 we present a systematic plot of the measured standard enthalpies of formation for all the 5d transition metal aluminides studied in this laboratory compared with calorimetric values for the corresponding 4d and 3d compounds. The enthalpies of formation of $LaAl_2$, OsAl, IrAl and PtAl were determined by Jung et al. [12] and Jung and Kleppa [13]. The heats of formation of the 4d aluminides were reported by Jung et al. [12], Jung and Kleppa [13] and Meschel and Kleppa [11]. The data for the 3d aluminides are cited from de Boer et al. [7] and Hultgren et al. [32]. Figure 1 exhibits some interesting trends. The absolute values of the enthalpies of formation of the 3d, 4d and 5d aluminides decrease systematically from the [Sc,Y,La] group to [Cr,Mo,W] and then increase fairly sharply to [Ni,Pd,Pt], i.e. there is a noticeable minimum at the [Cr,Mo,W] group. It is noteworthy that, of the three groups, the 4d compounds usually exhibit the most exothermic enthalpies of formation. In other words, in each triad of 3d, 4d and 5d transition elements, the magnitude of the enthalpy of formation increases from 3d to the corresponding 4d compound and then decreases from the 4d to the 5d aluminide. The only exception in this trend is the reversal at PdAl and PtAl.

In Fig. 2, the enthalpy of formation data for the 5d aluminides are compared with the corresponding data for 5d borides. If more than one compound was studied in any binary system, we selected to plot the value for the alloy with the larger Al/Me ratio. In Fig. 2 the heat of formation of LaB_6 was determined by Topor and Kleppa [33], the values for TaB_2, W_2B_5, ReB_2, Os_2B_5 and $IrB_{1.35}$ by Meschel and Kleppa [30, 31, 34] and the value for Pt_2B by Kleppa and Topor [35]. The

TABLE 2. Summary of standard enthalpies of formation of 5d aluminides (data in kJ (g atom)$^{-1}$)

Compound	$m = $ Al/Me	$\Delta H_m(1)$	$\Delta H_m(2)$	ΔH_f°
La$_3$Al$_{11}$	3.67	$4.5 \pm 0.6(6)$	$42.0 \pm 0.4(6)$	-37.5 ± 0.7
HfAl	1.0	$-8.1 \pm 1.8(6)$	$31.8 \pm 0.9(5)$	-39.9 ± 2.0
HfAl$_2$	2.0	$-12.8 \pm 0.9(6)$	$31.0 \pm 0.9(6)$	-43.8 ± 1.3
HfAl$_3$	3.0	$-9.7 \pm 0.4(5)$	$30.9 \pm 0.7(6)$	-40.6 ± 0.8
TaAl$_3$	3.0	$0.6 \pm 0.4(7)$	$30.5 \pm 1.2(5)$	-29.9 ± 1.3
Ta$_2$Al	0.5	$9.2 \pm 0.8(6)$	$29.1 \pm 1.4(5)$	-19.9 ± 1.6[a]
WAl$_4$	4.0	$15.2 \pm 0.4(6)$	$29.3 \pm 0.8(6)$	-14.1 ± 0.9
Re$_2$Al	0.5	$1.8 \pm 0.7(6)$	$31.4 \pm 0.5(6)$	-29.6 ± 0.9
Re$_4$Al$_{11}$	2.75	$-5.9 \pm 0.4(5)$	$28.6 \pm 1.4(6)$	-34.5 ± 1.5
Pt$_3$Al	0.33	$-32.0 \pm 1.8(5)$	$31.6 \pm 1.1(6)$	-63.6 ± 2.1
Pt$_2$Al$_3$	1.5	$-64.6 \pm 0.8(5)$	$31.9 \pm 0.9(5)$	-96.5 ± 1.2

[a]Indicative value.
Numbers in parentheses show numbers of experiments averaged.

TABLE 3. Comparison of ΔH_f° data for 5d aluminides with earlier experimental results and with predicted values from Miedema's semi-empirical model

| Compound	ΔH_f° (exptl.) (kJ (g atom)$^{-1}$) (this study)	ΔH_f° (exptl.) (kJ (g atom)$^{-1}$) (literature)	Method	ΔH_f° (predicted) (kJ (g atom)$^{-1}$)
La$_3$Al$_{11}$	-37.5	-42.7 (LaAl$_4$)	E.m.f. [26]	-47
		-35.3 (LaAl$_4$)	Calorim. [27]	
HfAl	-39.9	-46.3	Phase equil. [28]	-75
HfAl$_2$	-43.8	-48	Phase equil. [28]	-65
HfAl$_3$	-40.6	-42	Phase equil. [28]	-51
TaAl$_3$	-29.9	-36.4	Calorim. [9]	-30
		-23.7	Vapor pressure [29]	
Ta$_2$Al	-19.9[a]	-11.3	Vapor pressure [29]	-37
WAl$_4$	-14.1	$-$	$-$	-10
Re$_2$Al	-29.6	$-$	$-$	-24
Re$_4$Al$_{11}$	-34.5	$-$	$-$	-20
Pt$_3$Al	-63.6	-69.9	Calorim. [23]	-50
Pt$_2$Al$_3$	-96.5	-95.0	Calorim. [23]	-79

[a]Indicative value.
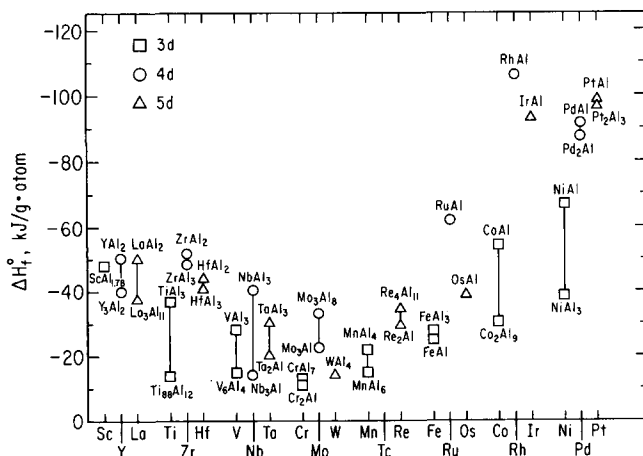
Fig. 1. Comparison of the standard enthalpies of formation for the 5d aluminides with similar data for the 3d and 4d aluminides.

standard enthalpy of formation of HfB$_2$ is cited from Johnson et al. [36].

It is evident from Fig. 2 that the systematic trends for the aluminides and borides differ in important respects, the aluminides showing the larger exothermic values for the late transition metals and the borides for the early transition metals. This occurs in spite of the fact that boron and aluminum are immediate neighbors in column III of the Periodic Table.

Figure 3 compares the data for the 5d aluminides with the enthalpies of formation of some 5d germanides. The enthalpy data for La$_5$Ge$_3$, Hf$_3$Ge$_2$, IrGe and PtGe were reported by Jung and Kleppa [37, 38] and the enthalpy of formation of ReGe$_2$ was measured by Searcy et al. [39]. While the data for the germanides are less complete than for the aluminides, interesting differences and similarities are evident. As noted already for the borides, the germanides are more exothermic than the aluminides for the early transition metals La and Hf
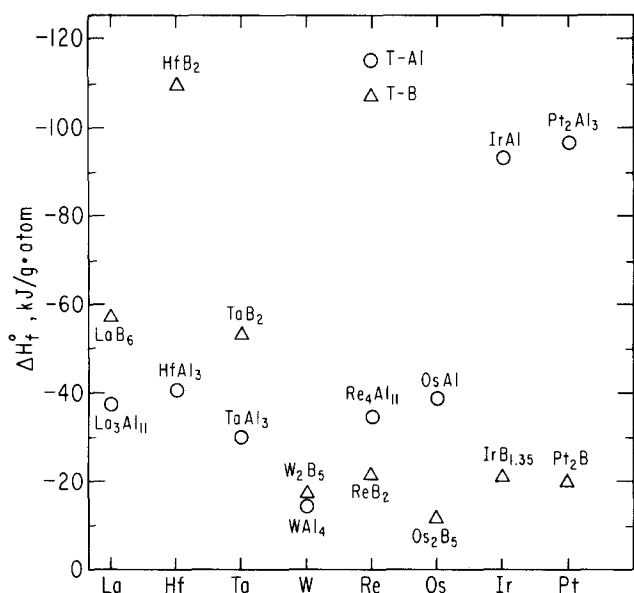
Fig. 2. Comparison of the standard enthalpies of formation for the 5d aluminides with similar data for the 5d borides.
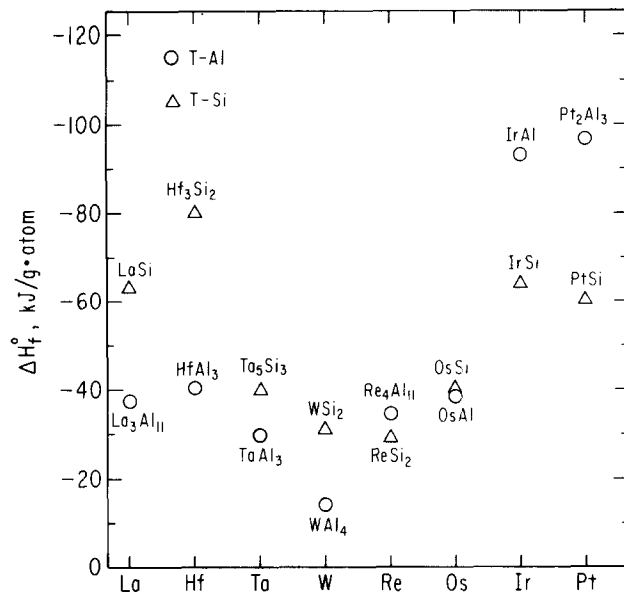

Fig. 4. Comparison of the standard enthalpies of formation for the 5d aluminides with similar data for the 5d silicides.
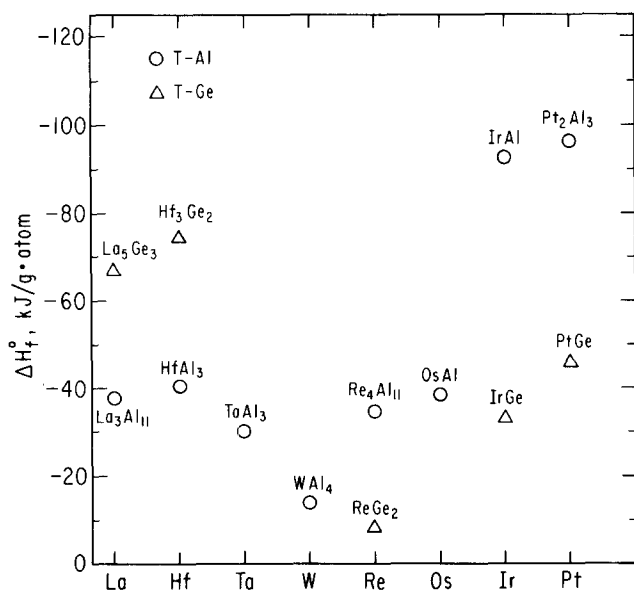

Fig. 3. Comparison of the standard enthalpies of formation for the 5d aluminides with similar data for the 5d germanides.

but much less exothermic than the aluminides for the late transition metals Ir and Pt. The reported value for $ReGe_2$ is even lower than our new value for WAl_4 and indicates, as for the aluminides, a minimum in $-\Delta H_f^\circ$ in the middle of the transition series. The observed trends are very similar to those found in the comparison between the 4d aluminides and germanides.

Figure 4 presents a comparison between our data for the 5d aluminides and the enthalpies of formation of 5d silicides. The heats of formation of Hf_3Si_2, OsSi, IrSi and PtSi were determined by Topor and Kleppa [40–42], the enthalpies of formation of Ta_5Si_3 and WSi_2 are cited from Robins and Jenkins [43] and the value

for $ReSi_2$ is quoted from Searcy and Finnie [44]. The enthalpy of formation of LaSi was measured by Samsonov et al. and quoted by Schlesinger [45]. The correlation of trends is very similar to that of the germanides in Fig. 3. We note a decrease in the magnitude of the enthalpies of formation from La to W and then an increase from Re to Pt. The silicides have the more exothermic values for the early transition metals while the aluminides are more exothermic for the late transition metals. It should be noted that the plotted value for OsSi is based on an interpolation and is hence very approximate [42]. The trends in the 5d aluminide–silicide graph are essentially the same as for the 4d aluminide–silicide comparison [11]. It is also worth noting that the pattern of an increase in the magnitude of the enthalpy of formation from 3d to 4d and a subsequent decrease to 5d is found for the aluminides, silicides and germanides. A comparison of the trends observed in Figs. 2, 3 and 4 suggests that the aluminides, silicides and germanides show a more similar thermodynamic behavior than the corresponding borides.

In our paper on the 4d aluminides we found no correlation between the observed enthalpies of formation and the difference in electronegativity between the two component elements [11]. The same situation holds for the 5d aluminides. For example, the electronegativity difference in PtAl and OsAl is nearly the same, while the heats of formation differ by a factor of about 2.5. This shows that the chemical bonding in the transition metal–Al compounds is covalent rather than ionic as already noted by Colinet et al. [46] and Pasturel et al. [5]. Similarly, the melting points of PtAl, $TaAl_3$, Re_4Al_{11} and $HfAl_3$ are within ±50 °C of each other; even so, the magnitude of the heat of formation

of PtAl is more than twice that of the other alloys. This lack of correlation between enthalpy of formation and melting point is similar to that found for the 4d aluminides.

Gelatt *et al.* [1] were the first to provide a detailed theoretical analysis of the important factors which contribute to the enthalpies of formation of transition metal–polyvalent metal systems. Further work along similar lines has been carried out by Manh *et al.* [4] and Pasturel *et al.* [5]. Pasturel's theory on 3d transition metal aluminides predicts a roughly parabolic dependence of the enthalpies of formation on the number of d electrons, with the weakest bonding in the middle of the series. This is consistent with our results for the 4d and 5d aluminides.

Gelatt *et al.* [1] conclude that there are two main contributions to the enthalpy of formation: (i) a negative (*i.e.* bonding) term which is due to the hybridization between the d band of the transition metal and the s and p bands of the polyvalent metal, and (ii) a positive (*i.e.* bond weakening) term which arises from the increase in the separation between the transition metal atoms caused by the alloying process. Hence there is a narrowing of the d band of the transition metal and a lowering of the cohesive energy of the alloy.

An analysis of the contributions of these two terms to the total energy of transition metal–aluminum alloys in the 4d transition metal series has led to the conclusion that the most negative enthalpies of formation should be found for alloys of Rh with Al (see ref. 1, fig. 6). It is very interesting to note that this is what we observe for the 4d aluminides. However, the experimental data for the 3d and 5d aluminides show that these alloys are different, since CoAl is less exothermic than NiAl and IrAl is less exothermic than PtAl. In other words for the 3d and 5d aluminides the most negative enthalpies of formation are found for Ni and Pt.

Acknowledgments

References

1 C. D. Gelatt, Jr., A. R. Williams and V. L. Moruzzi, *Phys. Rev. B, 27* (1983) 2005–2013.

2 M. O. Robbins and L. M. Falicov, *Phys. Rev. B, 29* (1984) 1333–1348.

3 A. Pasturel, P. Hicter and F. Cyrot-Lackmann, *J. Less-Common Met., 86* (1982) 181–186.

4 D. N. Manh, D. Mayou, A. Pasturel and F. Cyrot-Lackmann, *J. Phys. F, 15* (1985) 1911–1927.

5 A. Pasturel, D. N. Manh and D. Mayou, *J. Phys. Chem. Solids, 47* (1986) 325–330.

6 L. Brewer, *J. Phys. Chem., 94* (1990) 1196–1203.

7 F. R. de Boer, R. Boom, W. C. M. Mattens, A. R. Miedema and A. K. Niessen, *Cohesion in Metals. Transition Metal Alloys,* North Holland, Amsterdam, 1988.

8 O. Kubaschewski and G. Heymer, *Trans. Faraday Soc., 56* (1960) 473–478.

9 A. Neckel and H. Nowotny, *Int. Leichtmetalltag, 5th Internationale Leichtmetalltagung, 95* (1969) 72–76.

10 P. D. Desai, *J. Phys. Chem. Ref. Data, 16* (1987) 109–124.

11 S. V. Meschel and O. J. Kleppa, *J. Alloys Comp., 191* (1992) 111–116.

12 W. G. Jung, O. J. Kleppa and L. Topor, *J. Alloys Comp., 176* (1991) 309–318.

13 W. G. Jung and O. J. Kleppa, *Metall. Trans. B, 23* (1992) 53–56.

14 O. J. Kleppa and L. Topor, *Thermochim. Acta, 139* (1989) 291–297.

15 R. Hultgren, P. D. Desai, D. T. Hawkins, M. Gleiser, K. K. Kelley and D. D. Wagman, *Selected Values of the Thermodynamic Properties of the Elements,* American Society for Metals, Metals Park, OH, 1973, p. 154.

16 T. B. Massalski, H. Okamoto, P. R. Subramanian and L. Kacprzak (eds.), *Binary Alloy Phase Diagrams,* ASM International, Materials Park, OH, 2nd edn., 1990.

17 J. C. Schuster, *Z. Metallkd., 76* (1985) 724–727.

18 P. Villars and L. D. Calvert (eds.), *Pearson's Handbook of Crystallographic Data for Intermetallic Phases,* American Society for Metals, Metals Park, OH, 1986.

19 J. A. Bland and D. Clark, *Acta Crystallogr., 11* (1958) 231–236.

20 L. E. Edshammar, in A. Magneli, L. E. Edshammar and T. Dagerhamn (eds.), *Phase Analysis and Crystal Structure Studies on Binary Alloys of Aluminium with Transition Metals, Final Tech. Rep. 1,* Institute of Inorganic Chemistry, University of Stockholm, Sweden, 1963.

21 J. C. Schuster, *J. Less-Common Met., 98* (1984) 215–220.

22 A. H. Gomes de Mesquita and K. H. J. Buschow, *Acta Crystallogr., 22* (1967) 497–501.

23 R. Ferro, R. Capelli, A. Borsese and G. Centineo, *Atti Accad. Naz. Lincei, Cl. Sci. Fis. Mat. Nat., Rend., 45* (1968) 54–59.

24 R. Huch and W. Klemm, *Z. Anorg. Allg. Chem., 329* (1964) 123–135.

25 A. K. Niessen, F. R. de Boer, R. Boom, P. F. de Chatel, W. C. M. Mattens and A. R. Miedema, *Calphad, 7* (1983) 51–70.

26 V. I. Kober, I. F. Nichkov, S. P. Raspopin and V. A. Nauman, *Sov. Non Ferrous Met. Res., 5* (1977) 184–186.

27 G. Canneri and A. Rossi, *Chim. Gazz. Ital., 62* (1932) 202–211.

28 P. J. Spencer, in K. L. Komarek (ed.), *Hafnium: Physico-Chemical Properties of its Compounds,* Atomic Energy Review, No. 8, International Atomic Energy Agency, Vienna, 1981.

29 S. R. Schmidt and H. F. Franzen, *J. Less-Common Met., 116* (1986) 73–82.

30 S. V. Meschel and O. J. Kleppa, *J. Chim. Phys., 90* (1993) 349–354.

31 S. V. Meschel and O. J. Kleppa, *Metall. Trans.,* in press.

32 R. Hultgren, P. D. Desai, D. T. Hawkins, M. Gleiser and K. K. Kelley, *Selected Values of the Thermodynamic Properties of Binary Alloys,* American Society for Metals, Metals Park, OH, 1973.

33 L. Topor and O. J. Kleppa, *J. Chem. Thermodyn., 16* (1984) 993–1002.

34 S. V. Meschel and O. J. Kleppa, *J. Alloys Comp., 177* (1991) 159–166.

35 O. J. Kleppa and L. Topor, *J. Less-Common Met., 106* (1985) 269–276.

36 G. K. Johnson, E. Greenberg, J. L. Margrave and W. N. Hubbard, *J. Chem. Eng. Data, 12* (1967) 137–141.

37 W. G. Jung and O. J. Kleppa, *J. Less-Common Met., 169* (1991) 85–92.

38 W. G. Jung and O. J. Kleppa, *J. Alloys Comp. 176* (1991) 301–308.

39 A. W. Searcy, R. A. McNees, Jr. and J. M. Criscione, *J. Am. Chem. Soc., 76* (1954) 5287–5289.

40 L. Topor and O. J. Kleppa, *Z. Metallkd., 77* (1986) 65–71.

41 L. Topor and O. J. Kleppa, *Z. Metallkd., 79* (1988) 623–628.

42 L. Topor and O. J. Kleppa, *J. Less-Common Met., 167* (1990) 91–99.

43 D. A. Robins and I. Jenkins, *Acta Metall., 3* (1955) 598–604.

44 A. W. Searcy and L. N. Finnie, *J. Am. Ceram. Soc., 45* (1962) 268–273.

45 M. E. Schlesinger, *Chem. Rev., 90* (1990) 607–628.

46 C. Colinet, A. Bessound and A. Pasturel, *Z. Metallkd., 77* (1986) 798–804.